# Real-space scaling methods applied to the one-dimensional extended Hubbard model. II. The finite-cell scaling method

B. Fourcade and G. Spronken
*Département de Génie Physique, Ecole Polytechnique, Montréal, Québec, H3C3A7, Canada*
(Received 14 July 1983; revised manuscript received 12 January 1984)

The finite-cell scaling method is applied to the one-dimensional extended Hubbard Hamiltonian. The results obtained for the correlation functions show that, in the half-filled-band case, the hopping mixes the charge-ordered and the spin-ordered states. As with the real-space renormalization-group method, we find that the transition between these states is continuous and that the system, in the vicinity of the transition, is in a mixed charge-ordered—spin-ordered state.

## I. INTRODUCTION

In the preceding paper[1] (hereafter referred to as I) we have obtained the phase diagram of the extended Hubbard model in the half-filled-band regime using the real-space renormalization-group method. The phase diagram consists of two phases, the charge-ordered and the spin-ordered phases, and the transition across the boundary is a continuous transition. In the vicinity of the boundary, the ground state is a mixed charge-ordered—spin-ordered state, a result that differs from the broken-symmetry Hartree-Fock calculations.[2]

The purpose of the present paper is to confirm these conclusions by means of another real-space scaling technique: the finite-cell—scaling method developed by Sneddon.[3] In Sec. II the extended Hubbard model of I is rewritten in $\vec{k}$ space and the finite-cell—scaling method is introduced. The results are presented and discussed in Sec. III.

## II. MODEL AND METHOD

The one-dimensional extended Hubbard Hamiltonian of I may be written in $\vec{k}$ space as

$$H=2t\sum_{k\sigma}\cos k c^{\dagger}_{k\sigma}c_{k\sigma}+\frac{U}{n_s}\sum_{kk'qq'}\delta(k-k'+q-q')c^{\dagger}_{k\uparrow}c_{k'\uparrow}c^{\dagger}_{q\downarrow}c_{q'\downarrow}+\frac{G}{n_s}\sum_{\sigma\sigma'}\sum_{kk'qq'}\cos(k-k')\delta(k-k'+q-q')c^{\dagger}_{k\sigma}c_{k'\sigma}c^{\dagger}_{q\sigma'}c_{q'\sigma'}\ , \tag{1}$$

where $c^{\dagger}_{k\sigma}$ and $c_{k\sigma}$ are the usual creation and annihilation operators of an electron in the state $\{k,\sigma\}$. The first contribution to (1) is the Fourier transform of the first-neighbor hopping term. The quantity $2t$ stands for the half-width of the conduction band. The last two contributions come from, respectively, the intrasite ($U$) and the intersite ($G$) electron-electron—interaction energies. Here, $n_s$ is the number of sites of the chain whose lattice spacing has been set to unity. The sums run over all $k$'s belonging to the first Brillouin zone and $\delta(\cdots)$ is the Kroenecker $\delta$ modulo $2\pi$.

In the special case of $G=0$, on one hand, the Hamiltonian (1) reduces to the standard Hubbard model. On the other hand, in the saturated limit (all spins aligned in the same direction), (1) is equivalent to a spinless interacting fermion system, the analog of the Heisenberg-Ising linear chain. Both models have been exactly solved[4–6] with the result that, in the half-filled-band regime, the two models have singular behavior, the former at $U=0$ and the latter at $G=2|t|$. For both models it has been shown that this aspect of the exact solution is well reproduced by the finite-cell—scaling method.[7,8] In addition, the ground-state energy of the Hubbard model obtained with this method differs from the exact solution by less than 1%.[8] Accordingly, one would expect reliable results from its application to the extended Hubbard Hamiltonian (1), although there exists no exact result, in the general case, to check its reliability.

The finite-cell—scaling method essentially consists of solving the model exactly for finite blocks of increasing size. Quantities such as the gap are then obtained from the extrapolation of the finite-cell results to the infinite-chain system. Of course, on one hand, the larger the cell, the better the results of the extrapolation process. On the other hand, the calculations involved in the exact solution of the cell Hamiltonian rapidly become intractable as the number of sites increases, even when using all the symmetry properties of the Hamiltonian. There exists a technique, however, that makes it possible to partly overcome this difficulty: the Lanczos method, which has been extensively used in shell-model calculations,[9,10] and successfully applied to both spin-[11] and interacting-fermion systems.[7,8,12]

This method consists of constructing a tridiagonal representation for the matrix of the Hamiltonian by means of a repeated application of $H$. Starting with a normalized initial trial vector $|1\rangle$, the Lanczos procedure leads, after $m$ steps, to

 

$$H|1\rangle=\alpha_1|1\rangle+\beta_1|2\rangle$$
$$\vdots \qquad (2)$$
$$H|i\rangle=\beta_{i-1}|i-1\rangle+\alpha_i|i\rangle+\beta_i|i+1\rangle,\quad i=2,3,\ldots,m$$

where at each step $i$, the quantities $\alpha_i$ and $\beta_i$ are chosen such that the generated vector $|i+1\rangle$ is normalized and orthogonal to the previous ones. This process terminates when the complete basis (of, for instance, $M$ vectors) for this representation of $H$ is generated. It turns out that it is not necessary, however, to generate the entire basis to correctly reproduce the low-lying eigenvalues of $H$. It has been shown[9] that the lowest eigenvalue of the reduced $m\times m$ matrix ($m<M$) converges rapidly, as $m$ increases, toward the exact ground-state energy of the $M\times M$ matrix. It is this latter aspect of the method that makes the Lanczos procedure of real practical interest.

The selection of the initial vector $|1\rangle$ calls for a few remarks. There are four quantities which are left invariant by the Hamiltonian (1). These are the number of electrons $N$, the total momentum $K$, the total spin $\vec{S}$, and its projection along a given axis, $S_z$. These quantities all commute among themselves, and, accordingly, the starting vector, if chosen as being an eigenvector of $N$, $K$, $\vec{S}^2$, and $S_z$, will generate, through the Lanczos process, vectors all belonging to the subspace $\{n,k,s,s_z\}$, where $n$, $k$, $s(s+1)$, and $s_z$ stand for the eigenvalues of the corresponding operators. Such a choice for the initial vector makes a systematic study of the low-lying states of each subspace of the Hilbert space possible. Here, we are concerned with the absolute ground state, which has been proven by Lieb and Mattis[13] to lie within the $s=|s_z|$ subspace, where, for a given number of electrons, $|s_z|$ takes the lowest possible value. Accordingly, we shall start the Lanczos procedure with an initial vector that belongs to the $\{n,k,s=|s_z|,s_z\}$ subspace.

In general, it is difficult to construct a simultaneous eigenstate of the four operators $N$, $K$, $\vec{S}^2$, and $S_z$. We shall avoid this difficulty by following another approach.[9] Let us consider the following vector:

$$|1\rangle=c^\dagger_{k_1\sigma_1}c^\dagger_{k_2\sigma_2}\cdots c^\dagger_{k_n\sigma_n}|0\rangle\ , \qquad (3)$$

and the modified Hamiltonian

$$H'=H+\lambda[\vec{S}^2-S_z(S_z+1)]\ . \qquad (4)$$

In (3), $|0\rangle$ is the vacuum state, and $\lambda$, in (4), is a positive constant. The vector (3) is an eigenstate of $N$, $K$, and $S_z$ with eigenvalues $n$, $\sum k_i$, and $\frac{1}{2}\sum\sigma_i$ ($\sigma_i=\pm1$). Here, the eigenvalue of $S_z$ is assumed positive for the sake of simplicity. The additional term in (4) has no effect on states which belong to the $s=s_z$ subspace, while the other states with different value of $s$ are shifted toward higher energy. Accordingly, starting with (3), the Lanczos procedure using the modified Hamiltonian (4) yields a minimum-energy state that converges toward the ground state that belongs to the desired $s=s_z$ subspace.

The set of momenta involved in (3) is obtained from the boundary conditions. Here, we shall restrict ourselves to even numbers ($n_s$) of sites. Following Jullien and Martin,[12] we impose periodic boundary conditions for $n_s=4,8,12,\ldots,$

$$\exp(ikn_s)=1,\quad i^2=-1 \qquad (5a)$$

and antiperiodic boundary conditions for $n_s=2,6,10,\ldots,$

$$\exp(ikn_s)=-1\ . \qquad (5b)$$

The use of these alternate boundary conditions removes undesirable oscillations of the relevant physical quantities such as, for instance, the gap. Equations (5a) and (5b) assure that the free-electron half-filled-band Fermi momentum $|k_F|=\frac{1}{2}\pi$, for the infinite chain, is always included in the set of $k$'s.

## III. RESULTS

Applying the Lanczos method to the Hamiltonian (4) with the boundary conditions (5) yields the ground-state energy $\epsilon(n_s,n)$ for a chain of $n_s$ sites and $n$ electrons (the overlap integral $t$ has been taken equal to 1). The gap, defined as

$$\Delta(n_s)=\epsilon(n_s,\tfrac{1}{2}n_s+1)+\epsilon(n_s,\tfrac{1}{2}n_s-1)-2\epsilon(n_s,\tfrac{1}{2}n_s)\ , \qquad (6)$$

is plotted in Fig. 1 as a function of $1/n_s$ for $U=1$ and for several values of $G$. Computer limitations did not allow us to go beyond $n_s=8$. These curves, as well as similar curves obtained for other values of $U$ (not shown here), are sufficiently smooth to be fitted to a polynomial. In fact, they were fitted to a polynomial of degree $\frac{1}{2}n_s$ in $1/n_s$ with the result that the extrapolated value of the gap to the infinite chain is given by the following Lagrange expression:

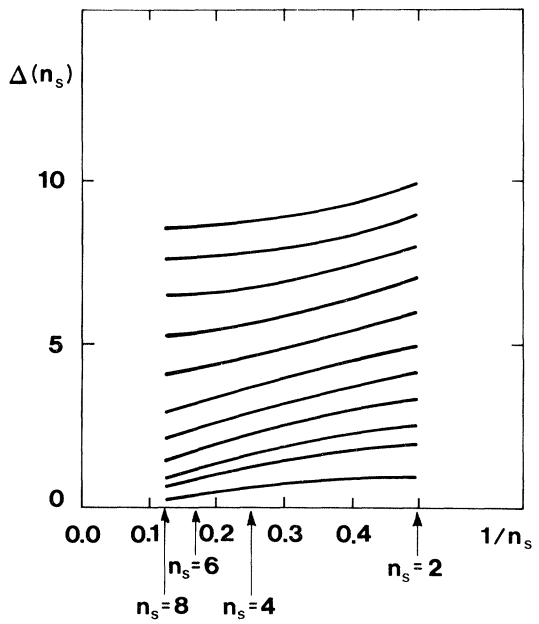


FIG. 1. Gap $\Delta(n_s)$ as a function of $1/n_s$ for $U=1$ and several values of $G$. From the top, the curves correspond to $G=2.75$, 2.50, 2.25, 2.00, 1.75, 1.50, 1.30, 1.10, 0.90, 0.80, and 0.30. Here $t=1$.

$$\Delta^{\infty}(n_s)=\sum_{p=1}^{n_s/2}\left[\prod_{q=1,q\neq p}^{n_s/2}\frac{1}{1-q/p}\right]\Delta(2p)\ . \tag{7}$$

In the atomic limit ($t=0$), the extended Hubbard model reduces, in real space (see I)

$$H=U\sum_i n_{i\uparrow}n_{i\downarrow}+G\sum_i n_i n_{i+1}\ , \tag{8}$$

which has been exactly solved by Bari.[14] The ground state corresponds to a charge-ordered state for $U<2G$ with energy $\frac{1}{2}n_sU$, and a spin-ordered state for $U>2G$ with energy $n_sG$. For a cyclic chain with an even number of sites, the values for the gap (single-particle excitation) are $\Delta=4G-U$ for $U<2G$ and $\Delta=U$ for $U>2G$. In Fig. 2, this exact result for $t=0$ is compared with the extrapolated value of the gap, $\Delta^{\infty}(8)$, obtained from (7) for $U=4$ and $t=1$. In this figure, we also give $\Delta(4)$, $\Delta(6)$, and $\Delta(8)$, together with, in the inset, $\Delta^{\infty}(4)$, $\Delta^{\infty}(6)$, and $\Delta^{\infty}(8)$, which show the dependence of the extrapolated results upon $n_s$ and the rate of convergence of these results towards the infinite chain. In Fig. 3 we have plotted the extrapolated value of the gap $\Delta^{\infty}(8)$ as a function of $G$ for both negative and positive values of $U$ ($t=1$). All these results clearly show the effects of the hopping. In the atomic limit the phase diagram has two well-defined

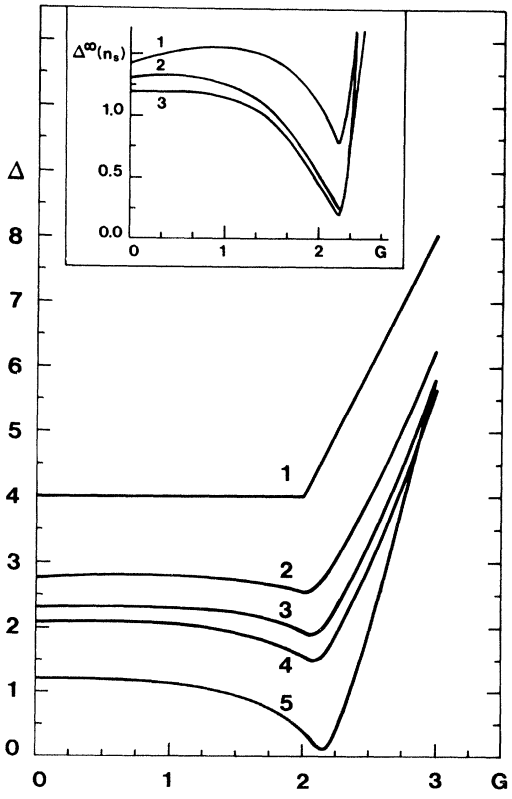


FIG. 2. Gap as a function of $G$ for $U=4$ and $t=1$. $\Delta$ stands for the gap $\Delta(n_s)$, for $n_s=2$ (curve 1), $n_s=4$ (curve 2), $n_s=6$ (curve 3), and $n_s=8$ (curve 4). The exact solution for $t=0$ and $\Delta(n_s=2)$ coincide. The extrapolated value of the gap $\Delta^{\infty}(n_s=8)$ is given by curve 5. The inset shows the rate of convergence of the extrapolated value of the gap. One has $\Delta^{\infty}(n_s=4)$ (curve 1), $\Delta^{\infty}(n_s=6)$ (curve 2), and $\Delta^{\infty}(n_2=8)$ (curve 3).

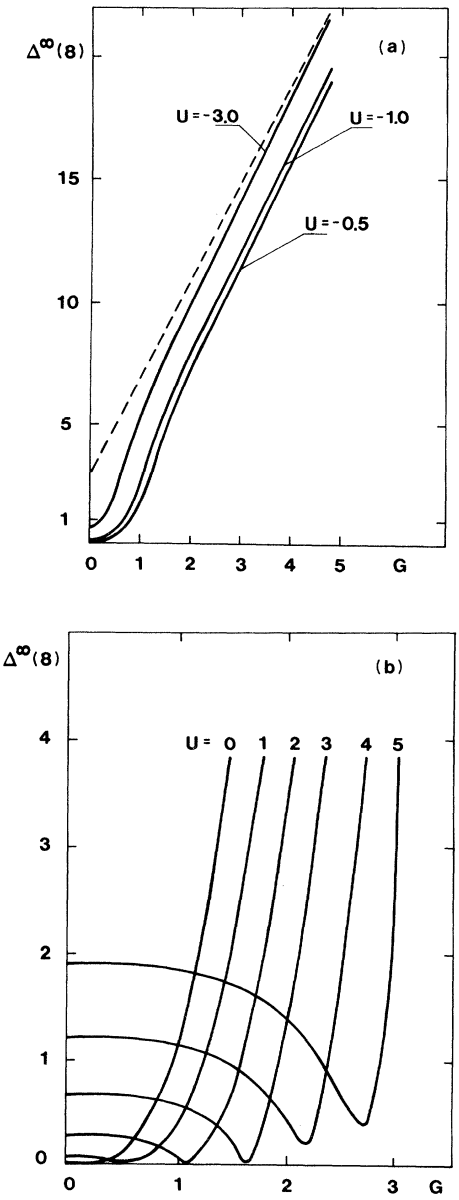


FIG. 3. Extrapolated value of the gap $\Delta^{\infty}(n_s)$ as a function of $G$ for both (a) negative and (b) positive values of $U$. In (a) the dashed line represents the gap in the atomic limit for the case $U=-3$. Here $n_s=8$ and $t=1$.

phases: charge ordered ($U<2G$) and spin ordered ($U>2G$), separated by the boundary $U=2G$. For $t\neq 0$, the gap (and its derivative) varies continuously as a function of $G$, which suggests that in the vicinity of the boundary (at which the derivative of the gap vanishes; see Fig. 4), the system is found in a mixed charge-ordered–spin-ordered state; that is, the hopping mixes both states. We shall show below that the values obtained for several correlation functions support this conclusion.

Table I shows that in the Lanczos procedure, correlation functions, such as the average number of doubly occupied sites, converge rapidly as a function of the number of Lanczos steps, which is an interesting result. As an example, in the case of the pure Hubbard model, with $t=0$,

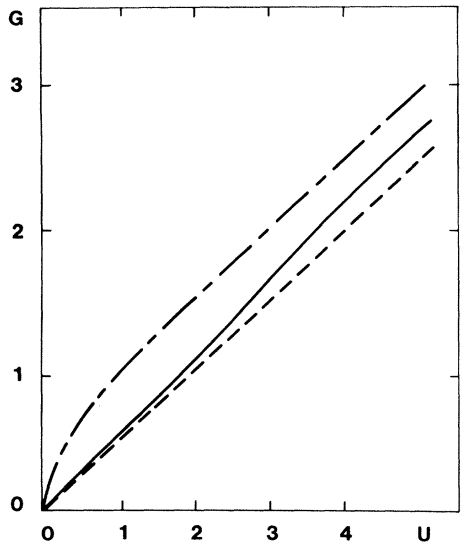


FIG. 4. $G$-$U$ phase diagram ($t=1$) for the range $U,G\geq 0$. The long-short dashed curve represents the real-space renormalization-group results, the dashed curve is the Hartree-Fock critical line, and the solid curve represents the present results.

the following quantities,

$$C_{\uparrow\downarrow}(n_s)=\frac{1}{n_s}\sum\langle n_{i\uparrow}n_{i\downarrow}\rangle\ , \tag{9a}$$

$$B_{\uparrow\downarrow}(n_s)=\frac{1}{n_s}\sum\langle n_{i\uparrow}n_{i+1\downarrow}\rangle\ , \tag{9b}$$

$$B_{\uparrow\uparrow}(n_s)=\frac{1}{n_s}\sum\langle n_{i\uparrow}n_{i+1\uparrow}\rangle\ , \tag{9c}$$

are $C_{\uparrow\downarrow}(n_s)=0$, $B_{\uparrow\downarrow}(n_s)=\frac{1}{2}$, and $B_{\uparrow\uparrow}(n_s)=0$ for all $n_s$, a result that shows that the ground state is $\cdots\uparrow\downarrow\uparrow\downarrow\cdots$. For $t\neq 0$, the results obtained for these quantities together with their extrapolated values [obtained from (7) in which $\Delta$ is replaced by $C_{\uparrow\downarrow}$, $B_{\uparrow\downarrow}$, or $B_{\uparrow\uparrow}$] are given in Fig. 5 as a function of $1/n_s$ for $U/t=2$ and 20 ($G=0$). These show that the hopping between sites reduces the local moment.

TABLE I. Ground-state energy $\epsilon(n_s,n)$ and the correlation function $B_{\uparrow\downarrow}(n_s)$ as a function of the Lanczos steps (here, $G=0.9$, $U=2$, $t=1$, $n_s=8$, and $n=4$; the size of the full matrix is $618\times 618$).

| Lanczos step | $\epsilon(n_s,n)$ | $B_{\uparrow\downarrow}(n_s)$ |
|---|---|---|
| 1 | −22.393 26 | 0.250 00 |
| 2 | −22.684 02 | 0.225 65 |
| 3 | −22.717 80 | 0.221 17 |
| 4 | −22.728 60 | 0.219 17 |
| 5 | −22.736 09 | 0.216 38 |
| 6 | −22.763 62 | 0.202 45 |
| 7 | −22.807 94 | 0.187 59 |
| 8 | −22.828 59 | 0.184 00 |
| 9 | −22.837 26 | 0.182 48 |
| 10 | −22.840 25 | 0.182 10 |
| 11 | −22.840 82 | 0.182 14 |
| 12 | −22.840 91 | 0.182 16 |
| 13 | −22.840 92 | 0.182 15 |

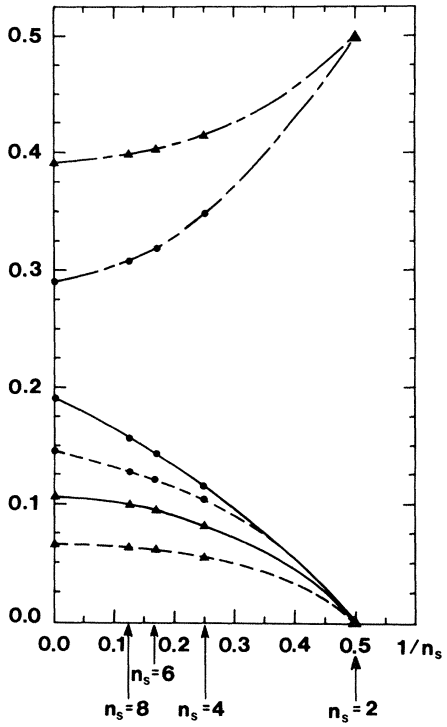


FIG. 5. Correlation functions as a function of $1/n_s$ for $G=0$, and for (●) $U/t=2$ and (▲) $U/t=20$. The dashed lines represent $C_{\uparrow\downarrow}(n_s)$, the solid lines represent $B_{\uparrow\uparrow}(n_s)$, and the long-short dashed curves represent $B_{\uparrow\downarrow}(n_s)$. The corresponding extrapolated values are given by the intersection with the vertical axis.

However, the ground state still has alternate up and down moments. All these results agree with the exact solution.[4]

In Fig. 6 we have plotted $C_{\uparrow\downarrow}(n_s)$ as a function of $1/n_s$ for $U=2$, $t=1$, and for several values of $G$ in the vicinity of the transition [which occurs at $G\sim 1.1$; see Fig. 3(b)]. The results are sufficiently well behaved to be extrapolated to the infinite-chain system. It is worth making, however, the following remarks. We have found that all the finite chains undergo a transition for $G\sim 1.1$ except the case $n_s=2$ (see Fig. 7). This is due to the fact that the allowed values of the individual momenta are, according to (5b), $k=\pm\pi/2$, and the band part of (1) vanishes identically; that is, the result does not differ from the atomic limit one ($t=0$) and the transition occurs[14] for $U=2G$. But this artifact has no consequence on the extrapolated results. For the range $1<G<1.1$, the curves of Fig. 6 are essentially straight lines, and the extrapolated values do not significantly differ whether we use $n_s=4$, 6, and 8 only, or $n_s=2$, 4, 6, and 8, where we choose the transition to happen artificially at $G=1.1$ in the $n_s=2$ case.

The results obtained for $C^{\infty}_{\uparrow\downarrow}(8)$, $B^{\infty}_{\uparrow\downarrow}(8)$, and $B^{\infty}_{\uparrow\uparrow}(8)$ are shown in Figs. 8 and 9 for $t=1$ and for two values of $U$ ($U=2$ and 5). Among these results, there are two cases where a jump in the curve can be clearly identified at the transition. This is not a surprising result since the extrapolation procedure is performed with only four values of $n_s$. Though the curves obtained (such as those of Fig. 6) are sufficiently smooth to be extrapolated to the infinite system, the set of $n_s$'s is not sufficiently numerous for one

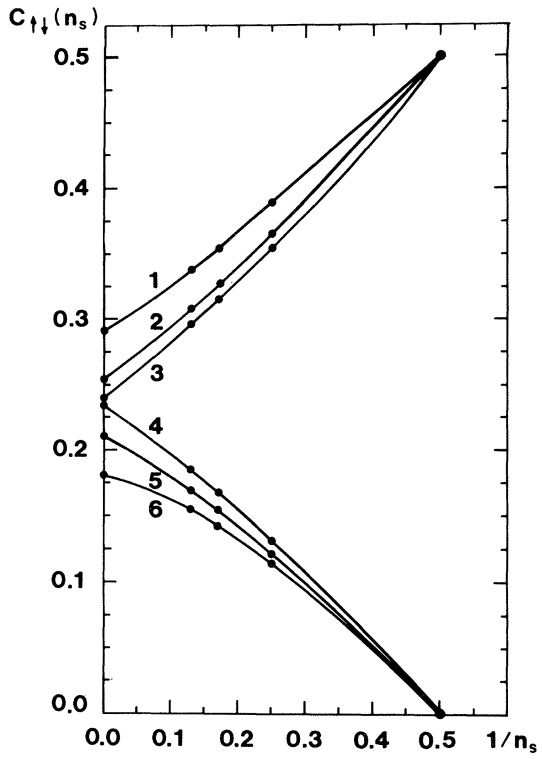


FIG. 6. Correlation $C_{\uparrow\downarrow}(n_s)$ as a function of $1/n_s$ for $U=2$ and several values of $G$. One has, respectively, 1, $G=1.5$; 2, $G=1.3$; 3, $G=1.2$; 4, $G=1.0$; 5, $G=0.7$; and 6, $G=0.0$. Here $t=1$.

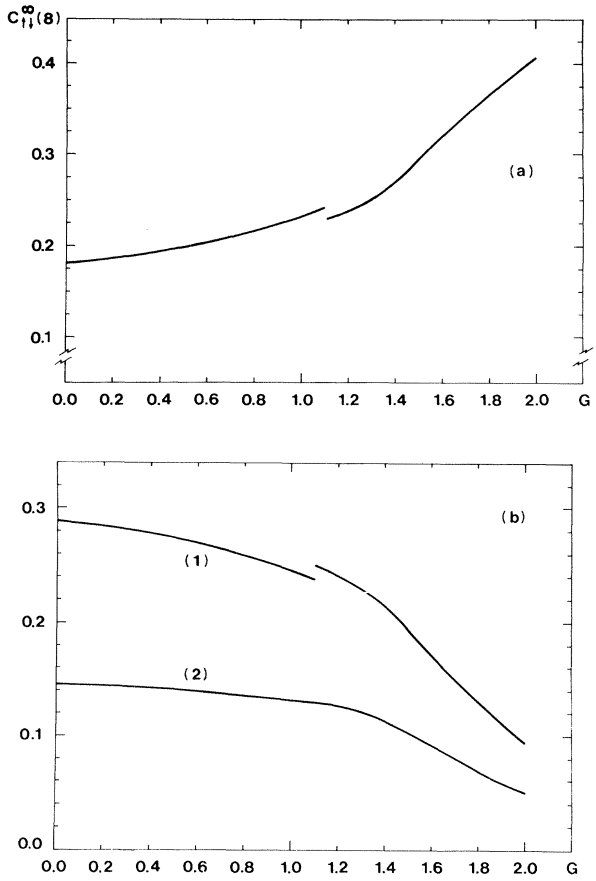


FIG. 8. Correlation functions as a function of $G$ for $U=2$ and $t=1$. (a) $C^{\infty}_{\uparrow\downarrow}(n_s)$. In (b), curve (1) refers to $B^{\infty}_{\uparrow\downarrow}(n_s)$ and curve (2) refers to $B^{\infty}_{\uparrow\uparrow}(n_s)$. Here $n_s=8$.

to expect very accurate results. In addition, the extrapolation is performed separately below and above the transition (see Fig. 7), and hence we expect to have a jump. Indeed, what is surprising is that the jump, if there is any, in the other curves is very small. Figures 8(a) and 9(a) show that, at least, the jump does not increase as $U$ increases, a result that is not expected if the jump has any physical meaning.

There is no obvious reason that could explain the fact that a jump is not systematically observed in all the curves, nor are there reasons which explain that, for a given $U$ (see Fig. 8), two curves have a jump while the other does not. Accordingly, we infer that the small jump in the curves of Fig. 8 stems from the lack of accuracy of the extrapolated results rather than from any physical effects. With the exception of these two cases, the general results are consistent with a second-order transition, and it is reasonable to conclude that the transition is continuous across the boundary. Thus the system is found, in the vicinity of the boundary, in a mixed charge-ordered—spin-ordered state.

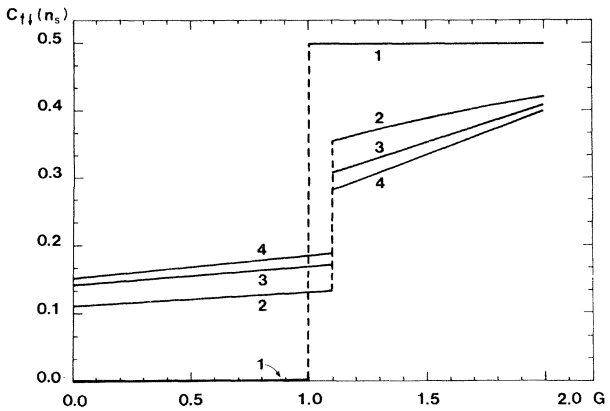


FIG. 7. Correlation function $C_{\uparrow\downarrow}(n_s)$ as a function of $G$ for 1, $n_s=2$; 2, $n_s=4$; 3, $n_s=6$; and 4, $n_s=8$. Here $U=2$ and $t=1$.

Finally, let us note, according to Fig. 3, that the gap vanishes for $U=G=0$ only, a result that clearly shows the singular behavior of the extended Hubbard model along both the $G$ and $U$ axes. The origin of the $G$-$U$ phase diagram is thus a fixed point,[11] in agreement with the results previously obtained with the real-space renormalization-group method (see I). We have shown[8] that the application of the finite-cell—scaling method to the pure Hubbard model ($G=0$ case) yields results which are in good agreement with the exact solution. We are presently studying the model along the $G$ axis (near $G=0$).

The results presented in this section call for a few additional remarks. The numerical results bear unavoidable computational runoff errors. We have, however, taken special care in performing the Lanczos calculations. Two different numerical schemes were used without giving significantly different results. In the first scheme, each vec-

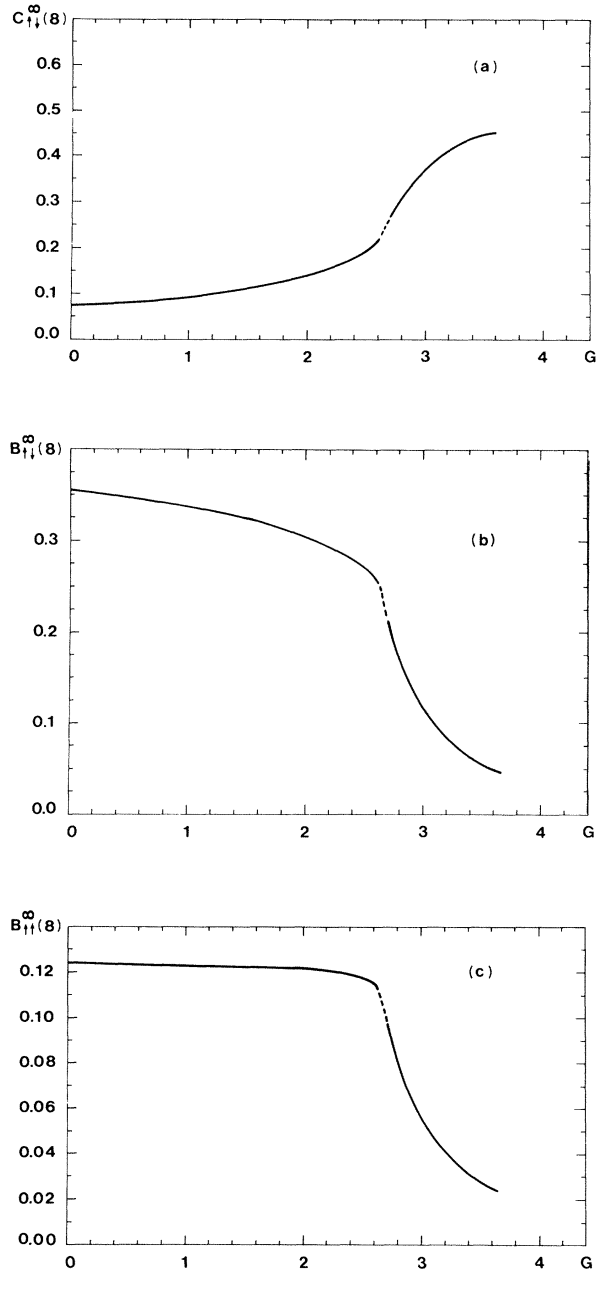


FIG. 9. Correlation functions as a function of $G$ for $U=5$ and $t=1$. One has (a) $C^{\infty}_{\uparrow\downarrow}(n_s)$, (b) $B^{\infty}_{\uparrow\downarrow}(n_s)$, and (c) $B^{\infty}_{\uparrow\uparrow}(n_s)$. Here $n_s=8$.

tor generated in (2) is orthogonalized to the two previous ones; in the second scheme, this vector is orthogonalized to all the previous ones. The extrapolation process is another possible source of errors. For the sake of clarity we have not put error bars on the curves of the figures. The results, however, all lie very close to the curves shown. Finally, our results are not numerous enough for us to perform a systematic study of the best fit of the curves. One could have fitted the curves of Fig. 6 with another function which would have given no jump. To show that the jump is indeed meaningless requires additional results. Computer limitations did not allow us to do so.

## IV. CONCLUSION

In this and the preceding paper (paper I) we have shown that the real-space renormalization-group and the finite-cell—scaling methods yield similar results. From the continuity of the correlation functions, one concludes that the extended Hubbard system, in the half-filled-band case, undergoes a continuous transition from a charge-ordered regime to a spin-ordered one. Hopping mixes the spin-ordered and charge-ordered states, and the system, in the vicinity of the boundary, is in a mixed charge-ordered—spin-ordered state. Both methods indicate that the gap varies continuously across the boundary. Only the finite-cell—scaling method, however, yields a continuous variation of the derivative of the gap. The results obtained with the real-space renormalization-group method indicate that the nature of the elementary excitations changes, at the boundary, from single-particle excitations to pair excitations. This is due to the fact that for the charge-ordered regime, the pairs are strongly bound (the binding energy is $U^{(\infty)}\rightarrow-\infty$; see I) and single-particle excitations are no longer possible. The results obtained with the finite-cell—scaling method behave differently, as single-particle excitations are always allowed (the binding energy is always finite).

In the atomic limit ($t=0$), the finite-cell—scaling method yields a gap $\Delta(n_s)$ which does not depend upon $n_s$, and the quantity $\Delta^{\infty}(n_s)$ obtained from (7) has the values $\Delta^{\infty}(n_s)=4G-U$ ($U<2G$, charge-ordered regime) and $\Delta^{\infty}(n_s)=U$ ($U>2G$, spin-ordered regime) for all sizes of the cell; that is, this method yields two phases separated by the boundary $U=2G$, in agreement with the exact solution.[14] This aspect of the phase diagram is also recovered using the real-space renormalization-group method (see I). The results, however, behave differently in the vicinity of the origin of the $G$-$U$ plane (see Fig. 4). According to the renormalization-group scaling equations,[15,16] the quantity $(U-2G)/t$ scales as $[(U-2G)/t]'=[(U-2G)/t]$ ($|U|$, $G\ll t$). Hence, the boundary is at $U=2G$. The phase diagram of Fig. 4 indicates that the finite-cell—scaling method alone is in agreement with the latter result. For the case $G=0$, we have shown[8] that this method yields results which are in good agreement with the exact solution.[4] Using the same technique, Uzelac[17] has also shown that the essential singularity of the pure Hubbard model is recovered with great accuracy. Hence, the finite-cell—scaling method gives reasonable results in the strong and weak coupling regimes.

The boundary obtained with the real-space renormalization-group method (see Fig. 4) departs significantly from the $U=2G$ line near the origin. As mentioned in I, this method yields $(U/t)'=(U/t)$ and $(G/t)'=\frac{1}{2}(G/t)$. The former result agrees with the scaling law while the latter does not. The quantity $(U-2G)/t$ does not scale properly and the method fails to reproduce the boundary $U=2G$. The fact that along the $U$ axis ($G=0$) this method is in agreement with the

scaling law may be fortuitous.[18] In addition, Dasgupta *et al.*[19] have shown that for the pure Hubbard system, this method yields an expression for the gap which does not agree with the exact solution even in the large-cell limit. For these reasons, we conclude that this method provides only a qualitative description of the properties of the system. It gives reasonable results in the strong coupling limit only.

## ACKNOWLEDGMENTS

We are grateful to A. Yelon for helpful discussions and to J. Currie for technical support. One of us (B.F.) acknowledges the France-Quebec Organization for financial support. This work was supported in part by the Natural Sciences and Engineering Research Council of Canada.

[1]B. Fourcade and G. Spronken, preceding paper, Phys. Rev. B 29, 5089 (1984).
[2]D. Cabib and E. Callen, Phys. Rev. B 12, 5249 (1975).
[3]L. Sneddon, J. Phys. C 11, 2823 (1978).
[4]E. Lieb and F. Wu, Phys. Rev. Lett. 20, 1445 (1968).
[5]R. Orbach, Phys. Rev. 112, 309 (1958).
[6]C. N. Yang and C. P. Yang, Phys. Rev. 147, 303 (1966); 150, 321 (1966); 150, 327 (1966); 151, 258 (1966).
[7]G. Spronken, R. Jullien, and M. Avignon, Phys. Rev. B 24, 5356 (1981).
[8]B. Fourcade and G. Spronken, Phys. Rev. B 29, 5012 (1984).
[9]R. Whitehead, A. Watt, B. J. Cole, and I. Morrison, *Computational Methods for Shell-Model Calculations* in *Advances in Nuclear Physics* (Plenum, New York, 1977), Vol. 9, p. 123.
[10]R. Whitehead, in *Theory and Application of Moment Method in Many Fermion Systems,* edited by J. B. Dalton, S. M. Grimes, J. P. Vary, and S. A. Williams (Plenum, New York, 1980).
[11]H. H. Roomany, H. W. Wyld, and L. E. Holloway, Phys. Rev. D 21, 1557 (1980).
[12]R. Jullien and R. M. Martin, Phys. Rev. B 26, 6173 (1982).
[13]E. Lieb and D. Mattis, Phys. Rev. 125, 164 (1962).
[14]R. A. Bari, Phys. Rev. B 3, 2662 (1971).
[15]V. J. Emery, A. Luther, and I. Peschel, Phys. Rev. B 13, 1272 (1976).
[16]V. J. Emery, in *High Conducting One-Dimensional Solids,* edited by J. T. Devreese, R. P. Evrard, and V. E. van Doren (Plenum, New York, 1979).
[17]K. Uzelac, J. Phys. A 17, L81 (1984).
[18]S. Sarker (private communication).
[19]C. Dasgupta and P. Pfeuty, J. Phys. C 14, 717 (1981).